Application of Recoil Techniques to Study of the Reactions $Ra^{226}(\alpha,4n)Th^{226}$, $Pb^{208}(\alpha,2n)Po^{210}$, and $Pb^{207}(\alpha,n)Po^{210}$†

JOHN R. MORTON, III,*‡ AND BERNARD G. HARVEY
Lawrence Radiation Laboratory, University of California, Berkeley, California

(Received December 4, 1961)

The ranges and angular distributions of the recoiling residual nuclei from the systems $Ra^{226}(\alpha,4n)Th^{226}$, $Pb^{208}(\alpha,2n)Po^{210}$, and $Pb^{207}(\alpha,n)Po^{210}$ have been examined to obtain information about the reaction mechanisms. The experimental angular distributions were compared with distributions calculated by a Monte Carlo method based upon the compound nucleus and statistical models. The results from the $Ra^{226}(\alpha,4n)$ reactions are in agreement with the calculations; the $Pb^{208}(\alpha,2n)$ and $Pb^{207}(\alpha,n)$ data require substantial contributions from direct-interaction mechanisms.

INTRODUCTION

A TECHNIQUE has been recently described by Donovan, Harvey, and Wade for study of the angular distributions of the recoiling residual nuclei from heavy-element nuclear reactions.[1] Their approach provides somewhat more detailed information about the mechanism of a reaction leading to a specific product than can be obtained from cross-section measurements. They also found that measurement of the ranges of the recoiling residual nuclei was quite helpful for interpreting the results.[2] The treatment included a Monte Carlo method for calculating the angular distributions of the recoiling product nuclei resulting from isotropic evaporation of neutrons from the compound nucleus. Certain of the reactions in their study seemed to be consistent with this mechanism while others did not. This work was done to test that treatment with additional reactions.

EXPERIMENTAL PROCEDURES

The targets were prepared by vacuum evaporation of radium chloride, Pb^{208}(96% enriched), Pb^{207} (71.5% enriched), and natural lead metal, onto 0.001-in.-thick aluminum foils. The thickness of the radium targets was determined by direct alpha counting; the targets used had a surface density of 1.2 ± 0.2 $\mu g/cm^2$. The thicknesses of the enriched lead targets were determined by chemical analysis using the dithizone method[3]; their thicknesses were 1.0 ± 0.2 $\mu g/cm^2$ for Pb^{208} and 0.5 ± 0.08 $\mu g/cm^2$ for Pb^{207}. The natural lead targets used for the range experiments were estimated, from the weight of lead vaporized, to contain 5.6 ± 0.5 mg/cm^2.

All the bombardments were done at the Crocker Radiation Laboratory 60-in. cyclotron.

The recoil angular distribution experiments followed the techniques described in reference 1. The method involved the use of target and catcher foils centered on the beam axis in an evacuated chamber. Following bombardment, the catcher foil was divided into concentric rings, and the collected recoil activites were measured by gross alpha count or alpha pulse-height analysis, depending upon the particular products.

The recoil angular distributions from the $(\alpha,4n)$ and $(\alpha,2n)$ reactions were corrected for the effect of beam scattering by the target and degrading foils. Such a correction was not made to the (α,n) data because of the larger limits of uncertainty. The $Pb^{207}(\alpha,n)$ data were corrected for the Po^{210} produced from a 25% Pb^{208} impurity in the target material.

The recoil range experiments were of two types: (a) The recoil products from the 1.2-$\mu g/cm^2$ Ra^{226} targets were stopped in low-pressure hydrogen and collected electrostatically on a horizontal catcher foil by a 600-v negative potential[4] and the catcher foil was then sectioned for counting; (b) the recoil range experiments with the natural lead targets used the "thick target" technique discussed in reference 2. This procedure involves the use of a foil stack composed of pairs of target and catcher foils. The average projected range of the recoils is obtained from the relation

$$\frac{\text{average range}}{\text{target surface density}}=\frac{\text{recoil activity in catcher}}{\text{total activity in both foils}}.$$

MONTE CARLO CALCULATIONS

The Monte Carlo calculations used for comparison with the experimental recoil angular distributions are essentially those discussed in reference 1, which have been reprogrammed in the FORTRAN language for use with the IBM 704 digital computer.

The calculation is based upon the compound nucleus and statistical models, and assumes that neutron evaporation is the dominant mode of deexcitation. The neutrons are assumed to be evaporated isotropically from the compound nucleus with an energy spectrum of the

† This work was performed under the auspices of the U. S. Atomic Energy Commission.

* Part of this work was submitted in partial fulfillment of the requirements of the Ph.D. degree in chemistry at the University of California, Berkeley, California.

‡ Present address, University of California Lawrence Radiation Laboratory, Livermore, California.

[1] P. F. Donovan, B. G. Harvey, and W. H. Wade, Phys. Rev. **119**, 218 (1960).

[2] B. G. Harvey, W. H. Wade, and P. F. Donovan, Phys. Rev. **119**, 225 (1960).

[3] E. B. Sandell, *Colorimetric Determination of Traces of Metals* (Interscience Publishers, Inc., New York, 1959).

[4] B. G. Harvey, Ann. Rev. Nuclear Sci. **10**, 235 (1960). (This review article contains many general references to recent recoil studies.)

form following Jackson[5]:

$$P(E_n)dE_n = E_n e^{-E_n/T} dE_n, \quad (1)$$

where $P(E_n)$ is the probability of emitting a neutron of energy between E_n and E_n+dE_n, and T is a parameter commonly called the "nuclear temperature." This calculation assumes that T is constant throughout the evaporation sequence.

The major assumptions and methods of the calculation described in reference 1 were retained; however, the technique for selecting the neutron energies differed. The neutron energies were randomly selected to fit the spectrum of Eq. (1) by the procedure outlined in the Appendix.

For each cascade considered, the neutron energy selection continues until there is insufficient excitation energy for further evaporation to occur. For the cases which lead to the particular reaction of interest, the angular distribution is calculated for the recoiling nuclei; for all other reactions, the total number of cases is recorded for each type.

The spectra of the evaporated neutrons produced by this method of energy selection are identical to those produced by the calculation of reference 1. The procedure described here makes more efficient use of the computer because every neutron chosen fits the spectrum of Eq. (1).

The recoil angular distributions were calculated with the energies and other parameters corresponding to conditions of the experiment. Usually, the calculations were made for 5000 cases of the reaction of interest. The following items of information were produced:

1. The number of recoil events for the reaction of interest, corrected for solid angle, in angular increments corresponding to a given combination of target-to-catcher distance and ring radii.

2. The total number of each type of neutron evaporation reaction which occurred.

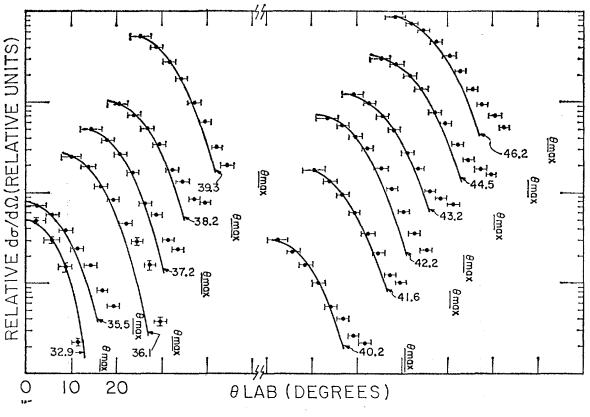

FIG. 1. Summary of experimental (points) and calculated (smooth curves) recoil angular distributions for $Ra^{226}(\alpha,4n)Th^{226}$. All the distributions begin at zero degrees with the same scale, but are displaced in the figure. The bombarding energy is indicated at the end of each calculated curve; the θ_{max} appropriate to that energy is marked immediately to the right in each case.

[5] J. D. Jackson, Can. J. Phys. **34**, 767 (1956).

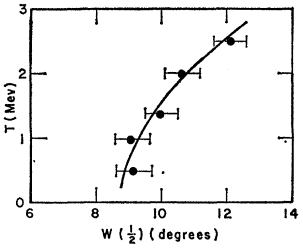

FIG. 2. Plot of the magnitude of the angle $W(\frac{1}{2})$ at which the relative differential cross section is reduced to half the forward value as a function of nuclear temperature. The calculation in this case is for the reaction $Bi^{209}(\alpha,2n)At^{211}$.

The general features of these angular distributions can be seen in Fig. 1. The shapes of the distributions are conveniently discussed in terms of $W(\frac{1}{2})$, the laboratory angle at which the relative differential cross section is reduced to one-half its value at zero degrees. The angles labeled θ_{max} are the maximum possible angles at which the recoils can be deflected by the neutrons at the particular bombarding energy.

Figure 2 shows that the value of T used for the calculations is relatively insensitive in its effect upon the resulting recoil angular distributions; however, it does affect the competition from other neutron evaporation reactions.[1] The cross-section data available for the reaction studied here were not sufficiently complete to define the competition from the various competing reactions in each case. Therefore, the value for T used in the calculations for each reaction was chosen by fitting the individual excitation functions using the procedure devised by Jackson.[5]

RESULTS AND CONCLUSIONS

The recoil angular distributions produced by the Monte Carlo calculations, with assumed isotropic neutron evaporation, form a basis for comparison with experiment. Agreement between the calculations and experiment lends support to the compound nucleus—statistical model description of these reactions. The recoil range measurements provide more direct information about the extent of momentum transfer. Normally, the formation of a compound nucleus is expected to lead to recoiling products with the maximum attainable kinetic energy; a few exceptions have been reported.[6] The range of the recoils is well-known to be an increasing function of their energy,[4] and, for recoils of low energy in stopping media of relatively much lighter atoms, the ranges of the recoils are expected to be proportional to their energy.[7]

The calculated and experimental recoil angular distributions will be compared below in summary plots of the angular distributions, and in plots of $(W\frac{1}{2})$ vs

[6] J. M. Alexander and L. Winsberg, Phys. Rev. **121**, 529 (1961).
[7] K. O. Nielsen, *Electromagnetically Enriched Isotopes and Mass Spectrometry* (Butterworth and Company, London, 1956).

TABLE I. Summary of experimental recoil angular distribution data[a]—$Ra^{226}(\alpha,4n)Th^{226}$.

E_α (Mev)	$W(\frac{1}{2})$[b] (degrees)	Relative $d\sigma/d\Omega$, for angles in degrees[c] 2.31	5.97	8.71	11.47	14.24	16.88	19.38	21.85	24.23	26.57
32.9	6.7	89	54	27	4.0						
35.5	8.6	35	29	19	12	7.5	4.0	2.7			
36.1	8.0	88	68	42	29	16	10	5.6	1.3		
37.2	8.3	62	46	32	20	9.0	7.0	3.7	2.8		
38.2	8.6	58	44	31	20	11	8.0	5.1	4.8		
39.3	8.6	90	68	47	31	16.5	10	5.3	3.3		
40.2	8.6	45	34	24	15	8.5	6.0	3.9	3.3		
41.9	8.7	98	74	51	34	19	11.5	6.6	5.5		
42.2	9.8	64	52	39	28	17.5	10.5	5.8	3.4	2.2	
43.2	9.7	44	36	26	18	10	6.8	3.8	3.2	2.7	
44.5	10.5	66	59	44	31	17	13	7.6	5.1	4.1	3.5
46.2	11.5	39	32	27	20	14	9.5	6.0	4.0	3.1	2.2

[a] Errors due to counting statistics are $\leqslant \pm 2\%$.
[b] The over-all error in $W(\frac{1}{2})$ is estimated to be $\leqslant \pm 0.5$ deg.
[c] The angles given here are determined by the mean radii of the catcher foil rings and a 4.0-cm target-to-catcher distance. The angular increments intercepted by the successive rings are 4.64, 2.66, 2.82, 2.70, 2.88, 2.42, 2.56, 2.40, 2.38, and 2.26 degrees. These increments correspond to spherical zones of relative area: 1.00, 1.48, 2.29, 2.81, 3.79, 3.76, 4.56, 4.77, 5.20, and 5.38.

$E_{\alpha\,\mathrm{c.m.}}+Q$, the energy available to the evaporated neutrons. The departure of the experimental points from the smooth calculated curves at wider angles is attributed to scattering from the surface of the target or from gas molecules in the evacuated chamber.

The recoil angular distribution and range results follow, grouped together for each reaction.

(a) $Ra^{226}(\alpha,4n)Th^{226}$

The experimental and calculated recoil angular distributions are compared directly in Fig. 1 and in terms of $W(\frac{1}{2})$ in Fig. 3. The agreement is very good over the entire energy range. The experimental recoil angular distribution data are summarized in Table I.

The general features of the plot of $W(\frac{1}{2})$ vs energy available for neutron kinetic energy have been interpreted[1] to mean: (1) that the momentum given to the residual nucleus increases as the excitation energy increases above the reaction threshold; (2) at energies near the peak of the excitation function, the neutrons have approximately the same energy; and (3) at still higher levels of excitation, the reaction occurs only when the emitted neutrons have relatively higher energies, due to competition from the reaction which causes an additional neutron to be evaporated.

A typical differential recoil range curve is shown in Fig. 4. These range curves were fitted to Gaussian distributions by use of probability plots from which the mean range, R_0, and the standard deviation, σ, could be determined.[8] The quality of fit of the data of Fig. 4 to the Gaussian is indicated in Fig. 5. In Fig. 6 the experimental Th^{226} recoil ranges in hydrogen are

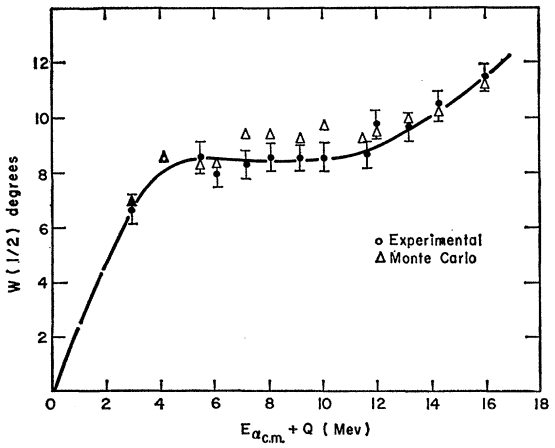

FIG. 3. Plot of $W(\frac{1}{2})$ as a function of $E_{\alpha\,\mathrm{c.m.}}+Q$, the energy available as kinetic energy of the emitted neutrons, for $Ra^{226}(\alpha,4n)Th^{226}$.

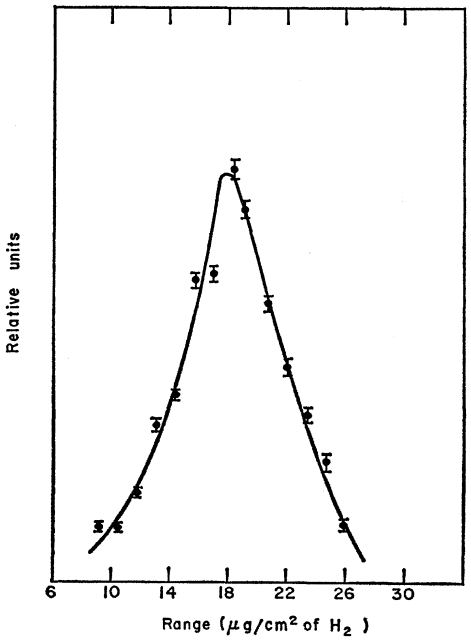

FIG. 4. Differential range curve for Th^{226} recoils in hydrogen; $E_\alpha = 41.6$ Mev.

[8] E. B. Mode, *The Elements of Statistics* (Prentice-Hall, Inc., Englewood Cliffs, New Jersey, 1941).

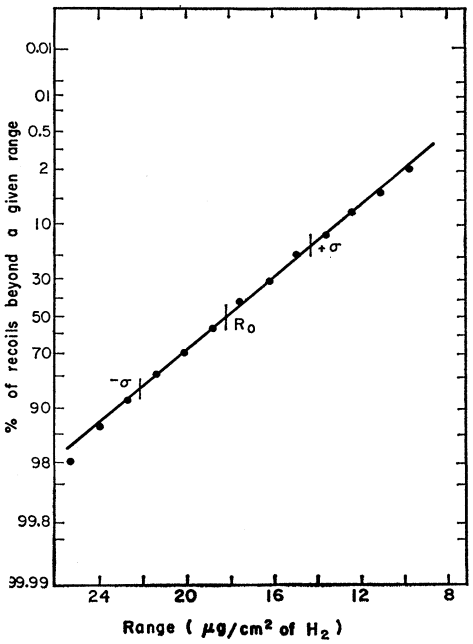

FIG. 5. Probability plot of Th^{226} recoil ranges in hydrogen for $E_\alpha=41.6$ Mev. The points $-\sigma$, $+\sigma$, and R_0 are indicated on the plot. In this case, $R_0=18.2$ $\mu g/cm^2$ and $\sigma=3.92$ $\mu g/cm^2$.

compared with a theoretical range-energy curve, for which the range is proportional to the recoil energy. The recoil energies, E_r, were based upon the assumption that a compound nucleus was formed.

The calculated recoil angular distributions were obtained using a nuclear temperature of 1.0 Mev, which was selected by Jackson fit[5] to the experimental excitation function of Vandenbosch and Seaborg.[9] The definition of the peak of the excitation function in this case

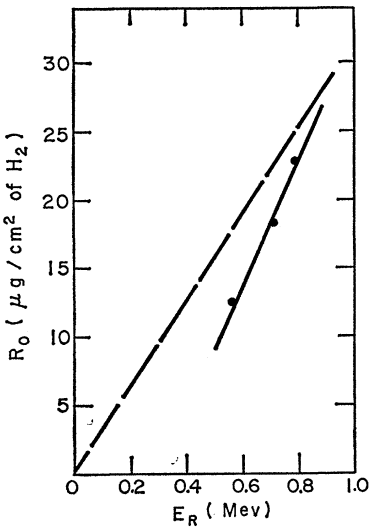

FIG. 6. Range of Th^{226} recoils in hydrogen as a function of the energy of the recoil (solid line). The broken line is the theoretical range-energy curve.

[9] B. Vandenbosch and G. T. Seaborg, Phys. Rev. **110**, 507 (1958).

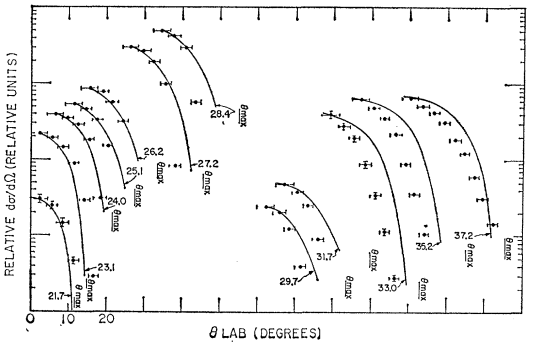

FIG. 7. Summary of experimental (points) and calculated (smooth curves) recoil angular distribution for $Pb^{208}(\alpha,2n)Po^{210}$. All the distributions begin at zero degrees with the same scale, but are displaced in the figure. The bombarding energy is indicated at the end of each calculated curve; the θ_{max} appropriate to that energy is marked immediately to the right in each case.

allowed 0.2- to 0.5-Mev latitude in selection of the temperature. The value used here is comparable to the value of 0.9 Mev obtained from the theoretical treatment of Cameron.[10]

The recoil range data of Fig. 6 define a range-energy curve which is reasonably consistent with the expectations for this magnitude of recoil energy. The reason for the deviation of the experimental ranges below the theoretical ones is not clear. A similar trend was reported by Valyocsik.[11] The approximate linearity of the data over the range of bombarding energy for which the reaction occurs is indicative of compound nucleus formation.

Vandenbosch and Seaborg suggested that this reaction proceeded by a compound nucleus mechanism based upon the approximately 500-mb maximum cross section. The recoil ranges and angular distributions appear to support this conclusion.

(b) $Pb^{208}(\alpha,2n)Po^{210}$

The experimental and calculated recoil angular distributions are compared directly in Fig. 7 and in terms of $W(\frac{1}{2})$ and the energy available for neutron kinetic energy in Fig. 8. Up to about 28 Mev, the agreement is fair, but at higher energies the experimental angular distributions are much more forward peaked than the calculated ones. This is similar to the $Bi(\alpha,2n)$ results of reference 2. The experimental recoil angular distribution data are summarized in Table II.

The Monte Carlo calculations used a nuclear temperature of 1.45 Mev obtained from the excitation function of John.[12] That excitation function has a maximum cross section of 1 b at about 30 Mev.

The recoil range data from natural Pb+He^4 are summarized in Fig. 9. Although the points of Fig. 9

[10] A. G. W. Cameron, Can. J. Phys. **36**, 1040 (1958).
[11] E. W. Valyocsik, thesis, University of California Radiation Laboratory UCRL-8855, 1959 (unpublished).
[12] W. John, Jr., Phys. Rev. **103**, 704 (1956).

TABLE II. Summary of experimental recoil angular distribution data[a]—$Pb^{208}(\alpha,2n)Po^{210}$.

E_α (Mev)	$W(\frac{1}{2})$[b] (degrees)	Relative $d\sigma/d\Omega$, for angles in degrees[c] 2.31	5.97	8.71	11.47	14.24	16.88	19.38	21.85	24.23
21.7	8.3	89	72	42	13					
23.1	10.5	91	80	62	36	12	1.2			
24.0	10.7	90	82	66	41	7				
25.1	9.7	96	83	59	27					
26.2	10.2	96	86	63	34					
27.2	9.6	98	85	60	30	2.5				
28.4	9.2	96	82	55	11					
29.7	8.8	97	80	50	16					
31.7	8.7	94	75	48	18					
33.0	8.2	92	68	46	21	8.4	2.8	0.7		
35.2	9.0	86	68	48	30	12.5	5.0	1.5		
37.2	10.0	85	67	54	40	24	16	8.0	4.0	1.9

[a] Errors due to counting statistics are $\leqslant \pm 2\%$.
[b] The over-all error in $W(\frac{1}{2})$ is believed to be $\leqslant \pm 0.5$ deg.
[c] The angles given here are determined by the mean radii of the catcher foil rings and a 4.0-cm target-to-catcher distance. The angular increments intercepted by the successive rings are 4.64, 2.66, 2.82, 2.70, 2.88, 2.42, 2.56, 2.40, 2.38, and 2.26 degrees. These increments correspond to spherical zones of relative area: 1.00, 1.48, 2.29, 2.81, 3.79, 3.76, 4.56, 4.77, 5.20, and 5.38.

are displaced to somewhat greater range than the $Bi(\alpha,2n)$ data of reference 2, there is a great similarity in the energy dependence of the recoil ranges for the high-energy side of the $(\alpha,2n)$ excitation function. These range data are fairly crude and do not define a linear-range energy curve for compound nucleus products. The estimated compound nucleus curve of Fig. 9 was drawn rather arbitrarily from a comparison with Fig. 7 of reference 2. The reason for the discrepancy between the bismuth and lead recoil ranges is not understood; it may be caused by the isotopic mixture of products, which could not be conveniently removed from the targets for resolution by alpha pulse-height analysis.

This evidence from both types of experiments indicates that, beginning at a bombarding energy of about 28 Mev, this reaction proceeds with approximately 10 to 20% of some mechanism other than formation of a compound nucleus which evaporates neutrons isotropically; the fraction of direct mechanism is estimated simply from the departure of the recoil ranges and angular distributions from the predicted compound nucleus case, as shown in Figs. 7 and 9. This would correspond to a 100- to 200-mb cross section for such a mechanism. The direct mechanism might cause the incident alpha particle to either knock a neutron out of the target nucleus or to be "stripped" of one neutron upon entering the nucleus; further de-excitation could then occur by evaporation of a second neutron.

Such reaction mechanisms are considered to be effective at the nuclear surface. The criterion which has been given for the enhanced probability for surface interactions is a "similarity" in the configurations of the initial and final states.[13] In these particular reactions that requirement might be achieved. The similarities between nuclei which differ by a pair of nucleons are well known.[14] An $(\alpha,2n)$ reaction is equivalent

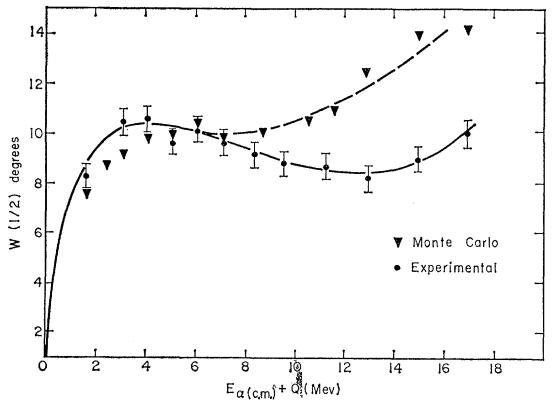

FIG 8. Plot of $W(\frac{1}{2})$ as a function of $E_{\alpha c.m.}+Q$ for $Pb^{208}(\alpha,2n)Po^{210}$. The solid line is drawn through the experimental points; the dashed line is drawn through the calculated points.

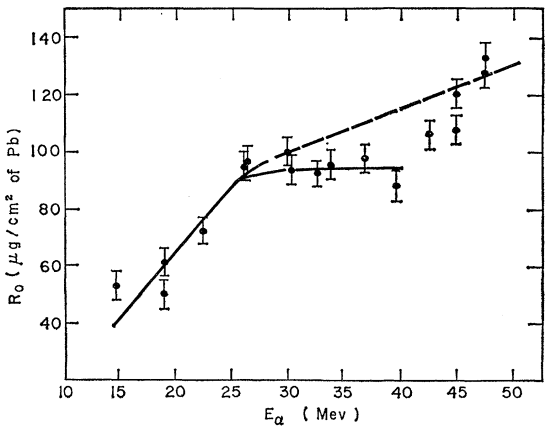

FIG. 9. Plot of mean recoil range as a function of bombarding energy for natural Pb+He^4. The solid line is drawn through the points representing probable products from the $(\alpha,2n)$ reaction. The broken line crudely represents the range curve that might be expected for a compound-nucleus mechanism.

[13] D. C. Peaslee, Ann. Rev. Nuclear Sci. **5**, 99 (1955).
[14] J. M. Blatt and V. F. Weisskopf, *Theoretical Nuclear Physics* (John Wiley & Sons, Inc., New York, 1952), p. 773.

to bringing a pair of protons into a nucleus. For the $Pb^{208}(\alpha,2n)Po^{210}$ reaction treated here and the $Bi^{209}(\alpha,2n)At^{211}$ reaction of reference 2, both the target and product lie on the $N=126$ closed shell; Pb^{208} is also located at the $Z=82$ shell closure. The abnormally large spacing of the neutron resonance levels in Pb^{208} is well established.[15] This location on the closed shells could lead to the expectation of having fair "purity" of shell-model states at or very near to the shell closure. This might explain the apparently large contribution from direct processes, although a 100- to 200-mb cross section for such a process is difficult to reconcile to direct interaction theories.

Serber's theoretical treatment of deuteron stripping, which was well supported by experiments, predicted a deuteron-stripping cross section for heavy elements of about 300 mb[16]; the alpha particle, being much more tightly bound than a deuteron, should be more difficult to break apart. Silva's experiments with alpha-particle stripping reactions of Bi^{209} gave an (α,d) cross-section of 2 to 3 mb and an (α,pn) cross-section of 18 to 20 mb.[17] The largest of these cross sections is a factor of 5 to 10 less than would give agreement with the apparent magnitude of the direct mechanism in the $(\alpha,2n)$ case.

Additional interesting information about this type of reaction would probably be obtained by applying these techniques to other $(\alpha,2n)$ reactions, particularly those involving nuclei away from closed shells.

(c) $Pb^{207}(\alpha,n)Po^{210}$

The experimental and calculated recoil angular distributions are compared in Fig. 10. The experimental data are summarized in Table III. For this reaction, the distributions cannot be compared conveniently in terms of $W(\frac{1}{2})$ because of the structure in some of the curves.

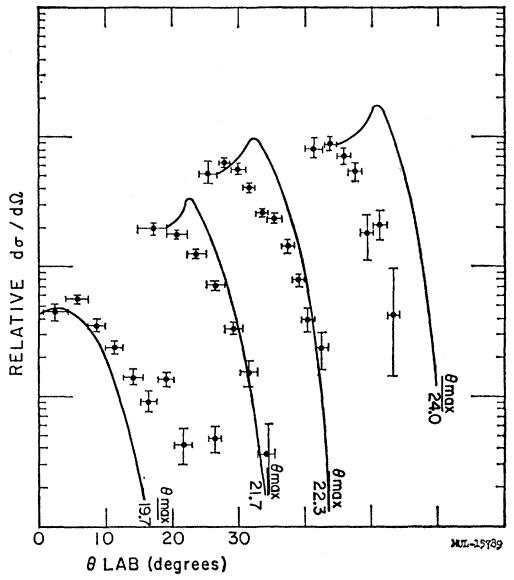

FIG. 10. Summary of experimental (points) and calculated (smooth curves) recoil angular distributions for $Pb^{207}(\alpha,n)Po^{210}$. All the distributions begin at zero degrees with the same scale, but are displaced in the figure. The bombarding energy is indicated at the end of each calculated curve; the θ_{max} appropriate to that energy is marked immediately to the right in each case.

Figure 10 shows that the experimental and calculated recoil angular distributions do not agree. The calculated curves show a maximum at the laboratory angle corresponding to 90° in the center-of-mass system; the experimental distributions are generally peaked forward and do not have the strong maximum.

The experimental excitation function of John[12] does not permit a precise specification of the nuclear temperature by the Jackson procedure; the calculations of Fig. 10 used a T of 1.4 Mev. Other calculations using $T=0.5$ and 2.0 Mev disagreed in the same way. In

TABLE III. Summary of experimental recoil angular distribution data—$Pb^{207}(\alpha,n)Po^{210}$.

E_α (Mev)	Relative $d\sigma/d\Omega$, for angles in degrees									
	2.32[a]	5.97	8.71	11.47	14.24	16.88	19.38	21.85	24.23	26.57
19.7	0.17[b]	0.22	0.13	0.09	0.05	0.03	0.05	0.02	0.0	0.02
21.7	1.71[c]	1.50	1.08	0.60	0.28	0.13	0.03			
	Relative $d\sigma/d\Omega$, for angles in degrees									
	1.54[d]	3.99	5.84	7.70	9.61	11.44	13.20	14.97	16.71	18.44
22.3	0.66[e]	0.80	0.73	0.52	0.33	0.30	0.18	0.10	0.05	0.03
24.0	0.59[f]	0.64	0.51	0.39	0.13	0.15	0.03			

[a] The angles given here are determined by the mean radii of the catcher foil rings and a 4.0-cm target-to-catcher distance. The angular increments intercepted by the successive rings are 4.64, 2.66, 2.82, 2.70, 2.88, 2.42, 2.56, 2.40, 2.38, and 2.26 degrees. These increments correspond to spherical zones of relative area: 1.00, 1.48, 2.29, 2.81, 3.79, 3.76, 4.56, 4.77, 5.20, and 5.38.
[b] Total error estimated $\leqslant 15\%$ to 14.24 deg.
[c] Total error estimated $\leqslant 8\%$ to 11.47 deg.
[d] The angles given here are determined by the mean radii of the catcher foil rings and a 6.0-cm target-to-catcher distance. The angular increments intercepted by the successive rings are 3.08, 1.80, 1.90, 1.84, 1.96, 1.68, 1.92, 1.76, 1.72, and 1.70 degrees. These increments correspond to spherical zones of relative area: 1.00, 1.47, 2.22, 2.84, 3.95, 3.94, 4.83, 5.37, 5.75, and 6.29.
[e] Total error estimated to be 21% for first point, $\leqslant 8\%$ for other points to 9.61 deg.
[f] Total error estimated to be $\leqslant 19\%$ to 7.70 deg.

[15] H. H. Barschall, C. K. Beckelman, R. E. Peterson, and R. K. Adair, Phys. Rev. **76**, 1146 (1949).
[16] R. Serber, Phys. Rev. **72**, 1008 (1947).
[17] R. J. Silva, thesis, University of California Radiation Laboratory UCRL-8678, 1959 (unpublished).

every case there was little correlation between the experimental and calculated maxima.

Recoil range experiments were not done for this reaction.

The disagreement between the experiments and calculations is probably evidence that the reaction occurs to a large extent by some direct interaction mechanism. The shift in the maximum in the recoil angular distributions to smaller angles would be consistent with such a mechanism.

Another possible reason for the disagreement is that the excitation energy in the (α,n) reaction might be insufficient to justify application of a statistical treatment. Since residual excitations of 5 to 6 Mev could be expected following evaporation of the neutron, this objection is not believed to be valid.

ACKNOWLEDGMENTS

We wish to thank the crew of the Crocker Laboratory Cyclotron for their assistance with the various experiments. The assistance of Dr. Paul F. Donovan, Ernest Valyocsik, Joe Cerny, and Leon Petrakis with several of the experiments is very much appreciated. The invaluable help from Walter Hutchinson and Douglas Brainard with modifications in the computer programming was also greatly appreciated.

APPENDIX. DETAILS OF NEUTRON ENERGY SELECTION SCHEME

An integral probability function was derived by integration of Eq. (1) to give

$$Z(N)=e^{-E_n/T}\left(\frac{E_n}{T}+1\right), \tag{2}$$

which is shown graphically in Fig. 11.

Because of the difficulty of solving for a unique value of E_n from a given randomly chosen value for $Z(N)$, the computation used a 2049-space table of $Z[(N-1)\Delta E]$, where ΔE is defined by

$$\Delta E=\frac{E_{\alpha\,\mathrm{c.m.}}+Q_1}{2048}; \tag{3}$$

$E_{\alpha\,\mathrm{c.m.}}$ being the energy of the projectile particle in the center-of-mass system, and $E_{\alpha\,\mathrm{c.m.}}+Q_1$ the maximum kinetic energy which the first neutron can have.

The energy probability table has a scale of uniform increments of energy associated with a nonuniform scale of probability. The probability "density" is related to the slope of the function at a given point. The problem is then to select a value of the probability function from that range which corresponds to the range of excitation energy available as kinetic energy to an evaporated neutron.

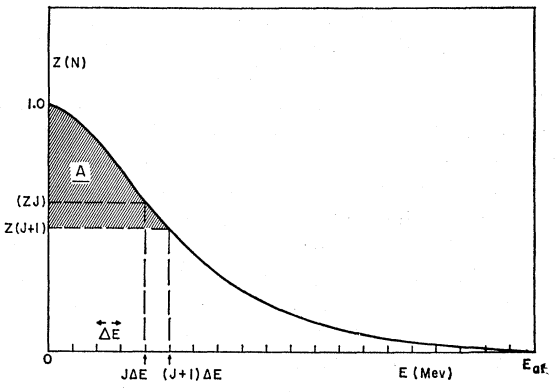

FIG. 11. Integral probability function for neutron energy selection. Scales are greatly exaggerated.

For describing the mechanics of the selection process, the following quantities are defined: $E_{ai}=E_{\alpha\,\mathrm{c.m.}}+Q_i$, the maximum energy available for kinetic energy to the ith neutron to be evaporated; E_{ri}—the energy removed as kinetic energy by the ith neutron; $\sum_i E_r$—the energy removed as kinetic energy by all the neutrons *evaporated previous to the* ith *one.*

The range of excitation energy available as kinetic energy to the ith neutron is defined by

$$J=(E_{ai}-\textstyle\sum_i E_r)/\Delta E, \tag{4}$$

which is rounded to an integral number. In Fig. 11 the cross-hatched region A corresponds to the range of excitation available for kinetic energy of the ith neutron. The random value of the probability function is obtained by multiplying the quantity $[1.0-Z(J+1)]$ by a random number between 0 and 1, then adding back $Z(J+1)$ in order to correctly set the absolute value for the random quantity $Z(R)$. The $Z(R)$ is located in the table of Z between two values $Z(N)$ and $Z(N-1)$. The randomly chosen kinetic energy for the ith neutron is then

$$E_{ri}=(N-1)\Delta E. \tag{5}$$

This procedure continues until there is insufficient excitation energy for further neutron evaporation.